Striatal cholinergic interneuron pause response requires Kv1 channels, is absent in dyskinetic mice, and is restored by dopamine D5 receptor inverse agonism

Tubert C[1,*], Paz RM[1,*], Stahl AM[1], Rela L[1,2], Murer MG[1,2]

[1] Universidad de Buenos Aires, CONICET, Instituto de Fisiología y Biofísica Bernardo Houssay, Grupo de Neurociencia de Sistemas, 2155 Paraguay St, Buenos Aires, 1121, Argentina.

[2] Universidad de Buenos Aires, Facultad de Medicina, Departamento de Ciencias Fisiológicas, 2155 Paraguay St, Buenos Aires, 1121, Argentina.

* Both authors contributed equally.

Rodrigo Manuel Paz, current address: Department of Neurology, UCSF, San Francisco, CA 94158, USA

Abstract

Striatal cholinergic interneurons (SCIN) exhibit pause responses conveying information about rewarding events, but the mechanisms underlying them remain elusive. Thalamic inputs induce a pause mediated by intrinsic mechanisms and regulated by dopamine D2 receptors, though the underlying membrane currents are unknown. Moreover, the role of D5 receptors (D5R) has not been addressed so far. We show that glutamate released by thalamic inputs in the dorsolateral striatum induces a burst in SCIN, followed by the activation of a Kv1-dependent delayed rectifier current responsible for the pause. Endogenous dopamine promotes the pause through D2R stimulation, while pharmacological stimulation of D5R suppresses it. Remarkably, the pause response is absent in parkinsonian mice rendered dyskinetic by chronic L-DOPA treatment but can be reinstated acutely by the inverse D5R agonist clozapine. Blocking the Kv1 current eliminates the pause reinstated by the D5R inverse agonist. In conclusion, the pause response is mediated by delayed rectifier Kv1 channels, which are tonically blocked in dyskinetic mice by a mechanism depending on D5R ligand-independent activity. Targeting these alterations may have therapeutic value in Parkinson's disease.

Highlights

- Thalamostriatal input triggers a burst followed by a pause in SCIN.
- Kv1, but not Kv7 or Kir2.2 channels, are necessary for the expression of the pause.
- D2R stimulation promotes, and D5R stimulation inhibits the pause.
- Thalamic bursts are not followed by a pause in SCIN from dyskinetic mice.
- D5R inverse agonism restores a Kv1-dependent pause response in dyskinetic mice.

Introduction

Dopamine (DA), released by neurons from the ventral tegmental area (VTA) and substantia nigra pars compacta (SNc), and acetylcholine (ACh), mainly released by striatal cholinergic interneurons (SCIN), are the main modulators of cortico-striatal circuits. Both types of neurons are tonically active, and their activity is altered by unexpected rewards or by the sensory cues that predict those rewards. These events evoke a burst in dopaminergic neurons coincident with a pause response in SCIN. The resulting increase in DA and decrease in ACh are critical for striatal-dependent learning and decision-making through modulatory effects on striatal "medium spiny" projection neurons (MSNs) (Cragg, 2006; Ding et al., 2010; Reynolds et al., 2022).

In vivo recordings show that the phasic response of striatal tonically active neurons (TANs, putative SCIN) to salient events typically involves a brief burst of action potentials followed by a short pause (Kimura et al., 1984; Aosaki et al., 1994a, 1994b; Apicella, 2007). The precise mechanisms underlying this response remain elusive. Evidence suggests the involvement of both dopaminergic and thalamic inputs in the generation of the pause. Neurons of the intralaminar nuclei of the thalamus, which send excitatory projections to the striatum, also respond to reward and salient stimuli, and the TANs pause is absent when the thalamus is locally inhibited (Matsumoto et al., 2001). Dopamine D2 receptor (D2R) antagonists or genetic elimination of D2R from cholinergic neurons have been shown to reduce the duration of the pause (Watanabe and Kimura, 1998; Ding et al., 2010; Kharkwal et al., 2016), implicating a direct contribution of D2R-mediated inhibition of SCIN. Additionally, e*x vivo* studies reveal heterogeneous responses of SCIN to stimulation of dopaminergic axons, with a more pronounced dopaminergic influence on the pause response in the dorsal versus the ventral striatum (Chuhma et al., 2014). Further evidence suggests that the pause in SCIN arises from intrinsic mechanisms activated by depolarization (Reynolds et al., 2004; Wilson and Goldberg, 2006; Sanchez et al., 2011). Experiments conducted in brain slices demonstrate that the pause that follows stimulation of SCIN excitatory inputs persists even after blocking GABA-A receptors, indicating the involvement of voltage (Kv) or calcium-dependent (KCa) potassium currents, with dopamine likely modulating these currents (Ding et al., 2010; Schulz and Reynolds, 2013; Zhang et al., 2018; McGuirt et al., 2022).

The importance of dopamine is underscored by the absence of pause in animals with chronic nigrostriatal lesions (Aosaki et al., 1994a). While reduced D2R stimulation may explain this, genetic elimination of D2R from cholinergic neurons reduces but does not eliminate the pause (Kharkwal et al., 2016), suggesting that additional factors are involved. SCIN also express dopamine D5 receptors (D5R), which have been recently linked to SCIN functional changes in parkinsonian animals (Paz et al., 2022).

However, their role in regulating phasic SCIN responses remains unaddressed, and whether alterations in D5R signaling contribute to the absence of pause in dopamine-depleted animals remains unclear.

Here, we report *ex vivo* studies showing that specific activation of intralaminar thalamostriatal inputs triggers a burst followed by a pause in SCIN. This pause requires the activation of an intrinsic delayed-rectifier current mediated by Kv1 channels, and is modulated by D2R and D5R. Furthermore, we found that the pause response is absent in parkinsonian mice with chronic L-DOPA treatment, but can be acutely reinstated by the inverse D5R agonist clozapine. Finally, the pause response reinstated by clozapine is abolished by blocking the Kv1 current, indicating that inhibition of constitutive D5R signaling releases this current from a tonic restraining effect, aligning with our prior findings (Paz et al., 2022).

Results

The timing of thalamic input interacts with SCIN intrinsic mechanisms to determine the duration of the pause response

To induce a pause in SCIN in response to thalamic activation, we injected an AAV2-CamKII-ChR2-YFP viral vector into the intralaminar nuclei of the thalamus in adult ChAT-Cre;tdTomato mice. We used these mice to facilitate the localization of SCIN in brain slices (Tubert et al., 2016). Four weeks later, we sacrificed the animals and made coronal slices of the striatum for *ex vivo* patch clamp recordings (Figure 1A). Histological analysis confirmed the site of AAV injection and the labeling of thalamostriatal projections (Figure 1B). We recorded SCIN in the cell-attached configuration and stimulated thalamic axons with 2 ms-long pulses of blue light at 20 Hz and 10 mW (Figure 1C). All the experiments were performed in the presence of picrotoxin (PIC, 100 µM) in the bath. When the stimulation elicited a minimal response (1 spike), the latency of the evoked spike decreased with the time separating the stimulus from the preceding spontaneous spike (Figure 1D-E). Thus, a stimulus arriving after an average baseline interspike interval (ISI) has elapsed produces a shorter latency response than when the stimulus arrives shortly after the preceding spontaneous spike (Figure 1E), as expected given the strong after-hyperpolarization (AHP) that follows SCIN spikes (Reynolds et al., 2004; Wilson and Goldberg, 2006). By increasing the number of pulses in the stimulation train, we obtained responses of 2 to 4 spikes ("bursts") followed by an interruption of SCIN firing, which were abolished by application of an AMPA receptor antagonist in the bath (firing rate during stimulus/baseline firing rate: PIC=3.611; PIC+CNQX=1.343; paired t test *p=0.0409; n=5 cells from 5 animals) (Figure 1F). Different train durations were required to evoke a given burst response across SCIN, probably relating to variability in the density of ChR2-expressing afferent fibers across experiments. To minimize the effect of this source of variability, we studied the pause duration as a function of the number of spikes in the burst evoked by

thalamic stimulation. The duration of the pause response increased with the number of spikes in the burst (Figure 1G), without changes in baseline ISI (Figure 1H), as expected if the pause depended on the recruitment of a depolarization-activated hyperpolarizing current. A pioneering *in vivo* study showed that the thalamic neurons presumptively driving the phasic response of SCIN show a burst followed by a pause that ends with a rebound of activity, in connection with reward-related events. This thalamic burst-pause response temporally coincides with the burst-pause response of the presumptive SCIN (Matsumoto et al., 2001). This suggests that a decrease of excitatory afferent activity may be necessary for the expression of the SCIN pause. To evaluate the effect of a second volley of excitatory inputs on the SCIN pause duration, we delivered a second thalamic stimulus train 350 ms after the end of the first stimulus. We found that the second stimulus train could terminate the pause, although its effect is delayed as more spikes are recruited in the burst by the first stimulus (Figure 1I-J). This is consistent with a graded recruitment of an intrinsic current that reduces the excitability of SCIN, delaying their response to the second stimulus.

The pause response to thalamic stimulation requires activation of Kv1 channels

In previous work we found that Kv delayed rectifier channels conformed by Kv1.3 and Kv1.1 subunits contribute to the sAHP current in SCIN of adult mice (Tubert et al., 2016). Moreover, a train of EPSPs evoked by thalamic afferents stimulation is followed by an AHP, which persists in the presence of the GABA-A receptor antagonist picrotoxin and is blocked by the Kv1.3 channel blocker margatoxin (Tubert et al., 2016). We asked whether this Kv1 current is recruited during the SCIN pause response. Both margatoxin (MgTx) at 30 nM – but not at 3 nM – and dendrotoxin (DTx, 100 nM, a Kv1.1 and Kv1.6 channel blocker) abolished the pause response without changing the spontaneous firing rate or the burst duration (Figure 2A-E). SCIN have a high reserve of Kv7 channels that limit EPSP summation but do not seem to contribute to the sAHP (Paz et al., 2018) or pause response (McGuirt et al., 2022) in adult mice. Consistent with these findings, the pause induced by thalamic stimulation was not reduced by the Kv7 channel blocker XE-991 (10 uM) (Figure 2F-I). Moreover, SCIN hyperpolarizations can be amplified by the recruitment of inwardly rectifying Kir2 channels, presumptively of the Kir2.2 subtype (Paz et al., 2021), which could then contribute to the pause response (Figure 2A). However, a low concentration of barium that preferentially blocks Kir2.2 channels (10 uM) had no effect on firing frequency, burst duration, or pause response of SCIN to thalamic stimulation (Figure 2F-I).

Overall, the data show that the Kv1 current is necessary for the expression of the pause that follows stimulation of thalamic inputs in SCIN of adult mice.

Activation of D5R reduces the pause generated in response to thalamic stimulation

Previous *in vivo* and *ex vivo* studies have shown that dopamine promotes the pause response through D2R-mediated actions (Aosaki et al., 1994a; Watanabe and Kimura, 1998; Deng et al., 2007; Ding et al., 2010), including inhibitory effects on Ih, which could be activated by the pause and contribute to its end (Deng et al., 2007; McGuirt et al., 2022). The pause shortens when D2R endogenous activation is blocked with D2-type receptor antagonists (Aosaki et al., 1994a; Watanabe and Kimura, 1998; Ding et al., 2010) or D2R are genetically eliminated (Kharkwal et al., 2016), and lengthens when D2R are overexpressed in SCIN (Gallo et al., 2022). In addition to D2R, SCIN express D5R that increase SCIN excitability by reducing the Kv1-mediated delayed rectifier current (Paz et al., 2021, 2022), shown above to be involved in the pause response. To assess whether D5R modulates the pause response induced by thalamic stimulation, we tested the effect of the D1/D5 receptor selective agonist SKF81297 in our *ex vivo* preparation. SKF81297 suppressed the pause without changing SCIN spontaneous firing rate (Figure 3A-E). The effect of SKF81297 was prevented by co-application of the selective D1/D5 receptor antagonist SCH23390, which had no effects by itself, ruling out tonic effects of DA through D5R (Figure 3A-E). Furthermore, we found a small effect of the selective D2R antagonist sulpiride, limited to the pauses that followed 4-spike bursts, supporting a modulatory role of D2R (Figure 3F-I). Previous studies suggested that synchronized SCIN bursts induce dopamine release through local effects mediated by nicotinic receptors located in dopaminergic terminals (Threlfell et al., 2012). Accordingly, the nicotinic receptor antagonist mecamylamine also reduced the pause that followed 4-spike bursts (Figure 3F-I). Presumably, endogenous levels of dopamine in the slice, produced by tonic release mechanisms or phasic cholinergic activation of dopaminergic terminals, are sufficient to stimulate D2R but not D5R.

Reduction of Ih current does not block the pause generated in response to thalamic activation

To evaluate if D5R stimulation reduces the pause response through effects on Ih current, we assessed if SKF81297 effect persisted in the presence of the HCN channel blocker ZD7288 (Figure 4A). We performed whole cell patch clamp recordings including ZD7288 in the recording pipette (Paz et al., 2021). ZD7288 blocked HCN channels as shown by the disappearance of the sag induced by hyperpolarizing steps (Figure 4B-C). Because HCN channel block also stopped spontaneous activity, we injected current through the electrode to induce spiking. In these conditions, thalamic input stimulation induced a burst-pause response. Additionally, the suppression of the pause by stimulation of D5R with SKF81297 was not prevented by Ih block (Figure 4D-G).

Our results, so far, extend previous work by showing that D5R can inhibit the pause response through effects that are independent of GABA-A receptors, burst amplitude, and Ih current, likely involving Kv1 current inhibition.

SCIN from L-DOPA-treated parkinsonian mice show reduced pause responses to thalamic activation

Previous *in vivo* work has shown that the pause response in SCIN is absent in an animal model of Parkinson's disease and is partially restored by acute administration of the dopamine receptor agonist apomorphine (Aosaki et al., 1994a). Chronic administration of L-DOPA to parkinsonian animals produces lasting changes in SCIN membrane excitability involving Kv1, Kir2, and likely, other currents (McKinley et al., 2019; Choi et al., 2020; Paz et al., 2021, 2022). Yet, whether chronic L-DOPA modifies the SCIN pause response has not been addressed before. We studied the pause response induced by thalamic afferents stimulation in SCIN from parkinsonian mice treated for 14 consecutive days with L-DOPA (12 mg/kg) or vehicle (Figure 5A). Mice unilaterally lesioned with 6-OHDA showed extensive loss of TH-positive neurons in substantia nigra pars compacta (Figure 5B), accompanied by marked parkinsonian-like motor impairment (Figure 5C-E). Moreover, these mice developed dyskinesia in response to L-DOPA administration, characterized by an abnormal involuntary movements score (AIM) that worsens after day 4 of treatment (Figure 5F). In previous studies, we have shown that the Kv1 current diminishes after lesioning nigral dopaminergic neurons and further suppressed when recorded 24 hours after the end of a chronic L-DOPA treatment (Paz et al., 2022). Cell-attached recordings performed 24 hours after the last L-DOPA challenge (OFF L-DOPA condition) showed that the pause is absent in SCIN from dyskinetic mice (Figure 5G-H), regardless of the burst duration (Figure 5J). Consistent with previous findings (Paz et al., 2021), the spontaneous firing rate was higher in SCIN recorded from mice in the OFF L-DOPA condition compared with sham mice (Figure 5I). In addition, inclusion of MgTx in the bath did not have any effect on pause duration, baseline firing rate and burst duration (Figure 5G-J), as expected following previous findings showing a lack of effect of MgTx on membrane excitability in the same animal model (Paz et al., 2022).

These results support that a reduction of the Kv1 current is involved in the loss of the pause response in dyskinetic mice.

Reducing D5R ligand-independent activity restores the SCIN pause response

In a previous study, we found that the physiological changes observed in SCIN of dyskinetic mice depend on an increase of ligand-independent activity of D5R (Paz et al., 2022). SCIN recorded in the parkinsonian

OFF-L-DOPA condition show an increase of membrane excitability that mimics changes acutely induced by SKF81297 in SCIN from control mice. This hyperexcitable phenotype reverts by acute administration of drugs that reduce D5R ligand-independent activity (i.e., inverse agonists, like clozapine or flupentixol), and by acutely reducing intracellular cAMP signaling. Interestingly, the hyperexcitability of SCIN recorded in the OFF L-DOPA condition is not further enhanced by SKF81297 or MgTx (Paz et al., 2022), suggesting D5R-cAMP-Kv1 inhibitory signaling is already working at full steam in these cells. Therefore, we speculated that, if suppression of the Kv1 current in parkinsonian mice causes the lack of pause response, D1/D5 inverse agonists should reinstate the pause. The atypical antipsychotic clozapine behaves as an antagonist of D1/D5 and other dopamine receptors when an agonist is present, but has inverse agonist effects on D5R in the absence of an agonist (Zhang et al., 2014). Remarkably, clozapine restores the pause in SCIN from dyskinetic mice without changing the firing rate and regardless of the burst duration (Figure 6A-E). As clozapine is not selective for D5R, we bathed the slices with the D1/D5 selective antagonist SCH23390, and with clozapine + SCH23390, to assess the involvement of D1/D5 dopamine receptors. We found that SCH23390 had no effect per se in the SCIN response to thalamic stimulation but prevented the restoration of the pause response by clozapine (Figure 6A-E). Moreover, to confirm that the pause restored by clozapine involves Kv1 channels, as is the case for naïve animals, we added clozapine and MgTx to the bath (Figure 6A). MgTx occluded the pause-restoring effect of clozapine (Figure 6B-E), indicating that the reduction of ligand-independent activity of D5R reinstates the Kv1 current in SCIN from OFF L-DOPA parkinsonian mice.

Discussion

While previous studies support the role of intrinsic membrane currents in the pause response of SCIN, the specific currents involved remain debated. Theories implicating deactivation of Ih current as its primary cause were refuted by experiments demonstrating pause induction after Ih current blockade when the resulting hyperpolarization is corrected by current injection (Zhang et al., 2018; present findings). Although Ih likely contributes to a rebound depolarization limiting pause duration (Deng et al., 2007; McGuirt et al., 2022). Further work suggested the involvement of a slow current mediated by Kv7 channels in juvenile mice (Zhang et al., 2018), which is developmentally downregulated and seems to not contribute significantly in the adult (McGuirt et al., 2022; present findings), though SCIN retain a high reserve of Kv7 channels sensitive to activators (Paz et al., 2018). Whether this Kv7 channel reserve is recruited under particular conditions not captured in our slice preparation remains to be determined. Previously, we found that Kv1 channels expressed by SCIN markedly modulate their excitability (Tubert et al., 2016). Heteromeric channels constituted by Kv1.3 and Kv1.1 subunits can be blocked by the

binding of a single MgTx molecule (Hopkins, 1998). In SCIN, MgTx enhances subthreshold EPSP summation and blocks the ensuing AHP (Tubert et al., 2016). The present study extends these findings by showing that specific blockers of channels constituted by Kv1.3 and Kv1.1 subunits suppress the pause that follows action potential bursts induced by thalamostriatal afferents in adult mice. Although SCIN express inwardly rectifying Kir2 channels capable of amplifying hyperpolarizations (Wilson, 2005; Paz et al., 2021), these channels do not contribute to the pause, likely because of insufficient membrane hyperpolarization to recruit Kir currents. Finally, *in vivo*, SCIN spontaneous firing rate synchronizes with excitatory synaptic input fluctuations (Krok et al., 2023). The SCIN phasic response could reflect burst-pause discharge synchronization with thalamic afferents, known to exhibit a burst-pause-rebound pattern in response to reward stimuli *in vivo* (Matsumoto et al., 2001). The effect of thalamic rebound activity on pause duration has not been examined before in brain slices. We observed that a second round of stimulation of thalamic afferents reduces the duration of the pause, although its impact is delayed by additional spikes in the initial SCIN burst, likely due to recruitment of a more robust Kv1 current.

Recent *in vivo* studies showed anticorrelated changes of DA and ACh striatal levels, not only during rewarded tasks but also during spontaneous behavior (Chantranupong et al., 2023; Krok et al., 2023). Several studies support that dopamine positively modulates the pause response of SCIN through D2R-mediated effects (Watanabe and Kimura, 1998; Ding et al., 2010; Kharkwal et al., 2016) and constitutive ablation of D2R from cholinergic neurons disrupts the anticorrelated DA-ACh signal during specific portions of an operant task (Chantranupong et al., 2023). However, striatal ACh transients persist and even increase after blockade of striatal DA receptors or lesion of nigrostriatal neurons, while they are reduced after intrastriatal infusion of glutamate receptor antagonists (Krok et al., 2023). Although these findings suggest that slow variations of striatal glutamate, rather than DA, control ACh release from SCIN at the space and time scales resolved by fiber photometry (Krok et al., 2023), they do not rule out a fine dopaminergic regulation of phasic SCIN responses to glutamatergic inputs, which could be embedded within broader modulations of DA and ACh levels. Our *ex vivo* data support that endogenous activation of D2R modulates the pause induced by thalamic afferents in SCIN. Moreover, we found that ambient DA in the slice does not modulate SCIN activity through D5R, but pharmacological stimulation of D1/D5 receptors markedly inhibited the pause response, likely through inhibitory effects of D5R on Kv1 channels. Overall, our data show that, in physiological conditions, Kv1 channels are necessary for the expression of the pause response in SCIN of adult mice, and that the pause can be modulated by D5R in addition to D2R. This D5R modulation may be relevant under conditions of phasic dopamine release producing synaptic concentrations of DA capable of activating the low affinity D5R (Figure 6F).

Learning deficits are believed to play a role in the development of Parkinson's disease symptoms. A recent study demonstrates that practice worsens the performance of previously learned motor skills in parkinsonian mice, while practice combined with therapeutic doses of L-DOPA prevents skill deterioration (Cheung et al., 2023). While this learning deficit may be due to the loss of dopamine, a possible contribution of SCIN dysfunction cannot be dismissed given that, in parkinsonian monkeys, the pause response of presumptive SCIN is lost and can be partially restored with apomorphine (Aosaki et al., 1994a). Our *ex vivo* studies provide a possible explanation for this pause response loss. We reported that the Kv1 current is diminished in parkinsonian mice and further suppressed 24 hours after the termination of a dyskinetogenic L-DOPA treatment (Tubert et al., 2016; Paz et al., 2022). Consistent with a key role of this current in pause generation, we find that the pause that follows a burst of spikes induced by stimulation of thalamostriatal afferents is markedly diminished in this animal model. Importantly, we previously reported that suppression of the Kv1 current in dyskinetic mice is caused by tonic effects of cAMP signaling, likely due to enhanced ligand-independent activity of D5R, as inverse agonists on D5R acutely restore the Kv1 current (Paz et al., 2022). Here, we find that clozapine, an atypical antipsychotic that antagonizes DA actions on D1-type and D2-type DA receptors, but behaves as an inverse agonist of D5R in the absence of an agonist (and DA levels should be very low in slices of 6-OHDA lesioned mice), reinstates the pause response of SCIN in dyskinetic mice. Remarkably, while the Kv1.3 blocker MgTx has no effect on SCIN in dyskinetic mice, as expected given the loss of Kv1 currents in this animal model (Paz et al., 2022), the pause reinstated by clozapine is suppressed by MgTx. This is consistent with previous findings showing that D5R inverse agonists reinstate the Kv1 current in dyskinetic mice (Paz et al., 2022), and supports the key role of the Kv1 current in the pause response and in the dysfunction observed in SCIN after DA neuron lesion and L-DOPA treatment (Figure 6F).

In conclusion, our study demonstrates that Kv1 channels are essential for the pause response of SCIN and its modulation by D5R in dopamine-intact animals. We also find that D5R dysregulation of Kv1 channels may contribute to the loss of this pause response in parkinsonian animals chronically treated with L-DOPA. Previously, we showed that D5R inverse agonists normalize the spontaneous firing pattern and membrane excitability of SCIN by restoring different membrane currents (Paz et al., 2022). The current findings reveal that D5R inverse agonists also restore the SCIN phasic responses to thalamic inputs, highlighting D5R ligand-independent activity as a key factor in SCIN dysregulation in the OFF L-DOPA condition.

Methods

Animals

Adult male and female mice (P60-250) allowing the identification of SCIN through cell type-specific expression of the fluorescent protein tdTomato (ChAT-Cre;tdT, for simplicity) were obtained as previously reported (Tubert et al., 2016; Paz et al., 2021). Briefly, ChAT-Cre;tdT mice were ChAT-Cre+/- and tdT+/-, and were obtained by crossing ChAT-Cre+/+ (B6;129S6-Chat tm2(cre)Lowl, stock 6410, The Jackson Laboratories; Rossi et al., 2011) and Rosa-CAG-LSL-tdTomato-WPRE+/+ mice (B6.CgGt(ROSA)26Sor tm14(CAG-tdTomato)Hze, stock 7914, The Jackson Laboratories). Up to six mice were housed per cage with water and food *ad libitum* and a 12:12 h light/dark cycle (lights on at 7:00 A.M.). Animals were cared for in accordance with institutional regulations (IACUC of the School of Medicine, University of Buenos Aires, 2023-891).

6-Hydroxydopamine Lesion

Under deep surgical anesthesia (isoflurane, 3% in O_2 for induction, 0.5-1% for maintenance) each mouse was mounted in a stereotaxic frame (Kopf Instruments; USA). The neurotoxin 6-hydroxydopamine-HBr (6-OHDA; Sigma Aldrich AB) was dissolved in 0.1% ascorbate-saline at the concentration 4 µg/µl (freebase). The skull was exposed, and a small hole was drilled at the desired injection site. The following stereotaxic coordinates were used to target the left medial forebrain bundle (MFB): 1 mm posterior (from Bregma), 1.1 mm lateral and 4.8 mm ventral from dura (Paxinos and Franklin, 2001). 1 µl was injected in adult mice (P90-110) at a rate of 0.5 µl/min using a 300 µm diameter cannula attached to a 25 µl Hamilton syringe controlled by a motorized pump (Bioanalytical Systems, USA). The injection cannula was left in place for six additional minutes before slowly retracting it. Littermates of lesioned mice received an injection of 0.1% ascorbate-saline in the MFB (sham group). After surgery, each mouse was daily weighted and received a subcutaneous injection of saline and an enriched diet. These cares continued until animals began to regain weight (7 to 20 days after surgery). To assess behavioral signs of parkinsonism, animals were subjected to extensive behavioral testing three weeks after 6-OHDA injection in three non-consecutive days (Figure 4A), during the light phase, by an investigator blind to treatment, as described in Escande et al., 2016. Briefly, spontaneous ipsilateral rotation in a novel open field (40 x 40 cm) is assessed using an automated video-tracking system (Anymaze). A rotation asymmetry index is computed by expressing the number of ipsilateral rotations relative to the total number of rotations. In the "cylinder test", each mouse is placed in a transparent acrylic cylinder (10 cm diameter and 14 cm high) and videotaped for five minutes. A limb use asymmetry score is computed by expressing the number of wall contacts performed with the forepaw contralateral to the lesion relative

to the total number of wall contacts performed with the forepaws. Finally, motor coordination is assessed in an accelerating rotarod (from 4 to 40 rpm in five minutes; Ugo Basile, Italy). The latency to fall from the rod is automatically recorded with a cut-off time of five minutes. Each animal was assessed five times with five-minute intertrial intervals in a single day.

L-DOPA Treatment

Mice were treated with 12 mg/kg of L-3,4-dihydroxyphenylalanine methyl ester hydrochloride (L-DOPA, Sigma Aldrich) combined with 12 mg/kg of benserazide (Sigma Aldrich). L-DOPA and benserazide were diluted in 0.9% saline solution. Abnormal involuntary movements (AIMs) were rated as previously described (Keifman et al., 2019). Briefly, AIMs rating started after 20 minutes of L-DOPA injection and mice were rated for 1 minute every 20 minutes during 2 hours. Each subtype of dyskinesia (oral, axial and forelimb) was scored on a scale ranging from 0 to 4 (where 0 = no dyskinesia; 1 = occasional dyskinesia displayed for <50% of the observation time; 2 = sustained dyskinesia displayed for >50% of the observation time; 3 = continuous dyskinesia; 4 = continuous dyskinesia not interruptible by external stimuli).

ChR2-EYFP adeno-associated vector injection

Anesthesia and surgical procedures were as indicated for the nigrostriatal lesions. A CaMKII-driven ChR2-EYFP expressing adeno-associated virus (rAAV2/CaMKII-hChR2(H134R)-EYFP-WPRE-PA) was injected in the thalamus at the following coordinates: -1.3 mm posterior from Bregma, 0.8 mm lateral and -3 mm ventral from dura (Paxinos and Franklin, 2001). 0.5 µl of viral vector was delivered using a glass micropipette (World Precision Instruments) pulled with a vertical glass puller (Narishige). Experiments were performed after at least 28 postoperative days (Figure 1A-B).

Patch Clamp Recordings

Twenty-four hours after the last L-DOPA shot, mice were anesthetized with isoflurane and decapitated for brain slicing. The brain was quickly removed, chilled in ice-cold low-Ca^{2+}/high-Mg^{2+}ACSF, and prepared for slicing. Coronal slices (300 µm) at the level of the striatum were cut with a vibratome (Pelco T series 1000, Ted Pella) and were incubated in low-Ca2+/high-Mg2+ artificial cerebrospinal fluid (ACSF) at 34ºC for 30 minutes and then at room temperature. ACSF composition was as follows (in mM): 125 NaCl, 2.5 KCl, 1.3$NaH_2PO_4 \cdot H_2O$, 26 $NaHCO_3$, 2 $CaCl_2$, 1 $MgCl_2$, and 10 glucose. For the low-Ca^{2+}/high-Mg^{2+} ACSF, 0.5 mM $CaCl_2$ and 2.5 mM $MgCl_2$ were used. Slices were transferred to a submersion-type chamber perfused by a peristaltic pump (Ismatec, Germany) with ACSF at a constant rate of 3ml/min; temperature in the recording chamber was set at 32ºC with a TC-344B temperature controller (Warner

Instruments). Cells were visualized using an upright microscope (Nikon Eclipse) equipped with a 40X water-immersion objective, DIC and fluorescence optics, and an infrared camera connected to a monitor and computer. Recording electrodes were made with borosilicate glass capillaries shaped with a puller (P-97, Sutter Instruments). Dorsolateral SCINs were recorded in cell-attached configuration with patch pipettes filled with intracellular solution (in mM): 20 KCl, 120 K-gluconate, 10 HEPES, 3 Na_2ATP, 0.3 NaGTP, 0.1 EGTA, 10 phosphocreatine and 2 $MgCl_2$, pH 7.3 adjusted with KOH. Recordings were amplified (Axopatch-1D; Molecular Devices), sampled at 20 kHz (Digidata 1322A, Molecular Devices) and acquired on a PC running pClamp 9.2 (Molecular Devices). In all the experiments, picrotoxin (100µM) was always present in the ACSF to block GABAergic transmission. Optogenetic stimulation was generated with a 447-nm light-emitting diode (Tolket, Argentina) and delivered through an optic fiber placed <300 um from the recorded cell. One to 20, 2-ms long pulses, at 20 Hz and 10 mW, were delivered 5 s after the initiation of the sweep, for 10 consecutive sweeps (Figure 1C). For experiments with a second pulse train, the second train was delivered 350 ms after the end of the first train. The second train contained 1-3 pulses (Figure 1I).

Pharmacological manipulations

Unless otherwise stated, reagents were purchased from Sigma (Argentina). Salts were purchased from Baker (Research AG, Argentina). Drugs were prepared as stock solutions, diluted in ACSF immediately before use, and applied through the perfusion system. The following stock solvents and final concentrations were used: distilled H_2O for BaCl (10µM), ZD7288 (30µM) and mecamylamine (10 µM, RBI); DMSO for CNQX (40µM, Tocris), picrotoxin (100µM), SKF81297 (2µM), SCH23390 (10µM), Sulpiride (10µM, Santa Cruz Biotechnology), XE991 (10µM) and clozapine (10µM, Rospaw Laboratory); and the manufacturer's recommended storage buffer (0.1% BSA, 100mM NaCl, 10mM Tris pH 7.5, 1mM EDTA) for margatoxin (MgTx 3nM and 30nM, Alomone Labs) and g-Dendrotoxin (100nM, Alomone labs).

Acquisition and analysis of electrophysiological data.

Data acquisition and analysis were performed with ClampFit (Molecular Devices, RRID: SCR_011323). GraphPad Prism version 8.00 for Windows (GraphPad Software, RRID:SCR_002798) and custom-made MATLAB (Mathworks, RRID: SCR_001622) routines were used for data analysis.

For each cell, 3 to 5 recordings were made, varying the number of light pulses delivered during the stimulation train. Each recording consisted of 10 sweeps with the same stimulus. Then, the recordings were analyzed by merging all the sweeps where the stimulation elicited the same number of spikes, regardless of the stimulation protocol. Only sweeps that triggered 1 to 4 spikes in response to the light were included in the analysis. The number of spikes in the burst was determined by the number of spikes

fired during the length of the stimulus plus 250 ms after the end of the stimulus. The pause was calculated as the time from the last spike of the burst triggered by the thalamostriatal input activation, and the following spike. The average baseline inter-spike-interval (ISI) was calculated taking into account all ISI collected during the five seconds preceding each stimulus. The burst duration was calculated as the time from the first to the last spike in the burst. To determine the influence of spontaneous spikes on evoked spiking, we plotted the time from the stimulus onset to the first spike in the burst (x2, for stimulations that evoked one spike) as a function of the time from the spike preceding the stimulus to the stimulus onset (x1). Each value was normalized to the average baseline ISI.

Each cell was recorded with only one pharmacological treatment. Most animals contributed with at least two neurons that received different drug treatments. For each experiment, control neurons were obtained from the same animals that contributed treated cells, plus a subset of cells from animals in which no cells were treated.

Perfusion

For confirmation of thalamostriatal projections to the striatum, ChAT-Cre;tdT mice were anesthetized with pentobarbital (100 mg/kg, i.p.), perfused through the ascending aorta with saline solution supplemented with heparin (2 U/ml, Rivero, Argentina) followed by 4% paraformaldehyde in 0.1 M phosphate buffer saline 0.1 M, pH 7.4 (PBS). Brains were removed, post-fixed for 24 hr in the same fixative, cryoprotected in 30% sucrose/PBS and cut. Sections containing the striatum and the thalamus were preserved in PBS with 0.1% sodium azide.

Immunohistochemistry

To confirm nigral dopaminergic lesions and the site of the AAV injection into the thalamus in mice used for acute slicing, tissue blocks containing thalamus and substantia nigra obtained after striatal slicing were fixed overnight in 4% paraformaldehyde in PBS, cryoprotected in 30% sucrose/PBS and cut at 30 µm with a sliding-freezing microtome (Leica). Sections containing the substantia nigra pars compacta were preserved in PBS with 0.1% sodium azide. For TH-immunoreactivity, sections were blocked for 2 hours at room temperature (PBS containing 5% NGS and 0.3% Triton X-100), incubated overnight with primary antibodies (mouse anti-TH, Chemicon, 1:1000, RRID: AB_2201528) at 4ºC, washed 3 times in 0.15% Triton X-100/PBS (PBS-T) and incubated with secondary antibodies conjugated to Alexa Fluor488 (Goat anti-mouse IgG, Invitrogen, 1:500, RRID: AB_138404) for 2 hours at room temperature. Sections were then washed 3 times in PBS-T and one time in PBS, mounted on glass slides with Vectashield (Vector) and coverslipped. For confirmation of the site of AAV injection, sections containing the thalamus were washed in PBS, mounted on glass slides with Vectashield (Vector) and coverslipped.

Image acquisition and analysis

Images of mounted sections were acquired with a Zeiss AxioImager M2 microscope with Neurolucida software (MFB Bioscience), with 10X, 20X or 40X objectives. Images were not modified after acquisition.

Statistical Analyses

Data were tested for normality and homoscedasticity with Anderson-Darling test and Spearman's rank correlation test respectively. Non-parametric tests were used when these criteria were not met. Statistical analysis details can be found in the figure legends and wherever numerical data is presented in the text. Significance level was set at $p<0.05$, and all data are expressed as mean ± SEM unless otherwise specified. GraphPad Prism and MATLAB routines were used for data analysis. Sidak or Dunn's corrections were applied for multiple comparisons.

Acknowledgments

The authors thank Graciela Ortega, Analía López Díaz, Agostina Presta, Verónica Risso, Lucía Garbini and Micaela Buscema for expert technical assistance in animal genotyping, histology and animal care and Juan Belforte for helpful discussions. We also thank the Rospaw Laboratory for their kind donation of clozapine. This study was supported by Fondo para la Investigación Científica y Tecnológica (FONCYT; Proyecto de Investigación Científica y Tecnológica [PICT] 2018-2738, 2019-2416, 2020-325 and 2022-42) and Universidad de Buenos Aires (UBACYT2018-305).

Author contributions

L.R., M.G.M., C.T. and R.M.P. designed the study. C.T. and R.M.P. performed the experiments. A.M.S. helped with the surgeries and animal care after the lesion. C.T., R.M.P., L.R., and M.G.M. wrote the manuscript.

References

Aosaki T, Graybiel AM, Kimura M (1994a) Effect of the nigrostriatal dopamine system on acquired neural responses in the striatum of behaving monkeys. Science 265:412–415 Available at:

http://www.ncbi.nlm.nih.gov/pubmed/8023166 [Accessed July 8, 2015].

Aosaki T, Tsubokawa H, Ishida A, Watanabe K, Graybiel AM, Kimura M (1994b) Responses of tonically active neurons in the primate's striatum undergo systematic changes during behavioral sensorimotor conditioning. J Neurosci 14:3969–3984 Available at: https://pubmed.ncbi.nlm.nih.gov/8207500/ [Accessed May 31, 2024].

Apicella P (2007) Leading tonically active neurons of the striatum from reward detection to context recognition. Trends Neurosci 30:299–306 Available at: https://pubmed.ncbi.nlm.nih.gov/17420057/ [Accessed May 31, 2024].

Chantranupong L, Beron CC, Zimmer JA, Wen MJ, Wang W, Sabatini BL (2023) Dopamine and glutamate regulate striatal acetylcholine in decision-making. Nat 2023 6217979 621:577–585 Available at: https://www.nature.com/articles/s41586-023-06492-9 [Accessed May 31, 2024].

Cheung THC, Ding Y, Zhuang X, Kang UJ (2023) Learning critically drives parkinsonian motor deficits through imbalanced striatal pathway recruitment. Proc Natl Acad Sci U S A 120 Available at: /pmc/articles/PMC10041136/ [Accessed May 31, 2024].

Choi SJ, Ma TC, Ding Y, Cheung T, Joshi N, Sulzer D, Mosharov E V., Kang UJ (2020) Alterations in the intrinsic properties of striatal cholinergic interneurons after dopamine lesion and chronic L-DOPA. Elife 9:1–24 Available at: https://pubmed.ncbi.nlm.nih.gov/32687053/ [Accessed May 31, 2024].

Chuhma N, Mingote S, Moore H, Rayport S (2014) Dopamine neurons control striatal cholinergic neurons via regionally heterogeneous dopamine and glutamate signaling. Neuron 81:901–912 Available at: https://pubmed.ncbi.nlm.nih.gov/24559678/ [Accessed May 31, 2024].

Cragg SJ (2006) Meaningful silences: how dopamine listens to the ACh pause. Trends Neurosci 29:125–131 Available at: http://www.ncbi.nlm.nih.gov/pubmed/16443285 [Accessed July 9, 2015].

Deng P, Zhang Y, Xu ZC (2007) Involvement of I(h) in dopamine modulation of tonic firing in striatal cholinergic interneurons. J Neurosci 27:3148–3156 Available at: http://www.ncbi.nlm.nih.gov/pubmed/17376976 [Accessed July 13, 2015].

Ding JB, Guzman JN, Peterson JD, Goldberg JA, Surmeier DJ (2010) Thalamic gating of corticostriatal signaling by cholinergic interneurons. Neuron 67:294–307 Available at: http://www.pubmedcentral.nih.gov/articlerender.fcgi?artid=4085694&tool=pmcentrez&rendertype=abstract [Accessed July 11, 2014].

Escande MV, Taravini IRE, Zold CL, Belforte JE, Murer MG (2016) Loss of homeostasis in the direct

pathway in a mouse model of asymptomatic parkinson's disease. J Neurosci 36.

Gallo EF, Greenwald J, Yeisley J, Teboul E, Martyniuk KM, Villarin JM, Li Y, Javitch JA, Balsam PD, Kellendonk C (2022) Dopamine D2 receptors modulate the cholinergic pause and inhibitory learning. Mol Psychiatry 27:1502–1514 Available at: https://pubmed.ncbi.nlm.nih.gov/34789847/ [Accessed May 31, 2024].

Hopkins W (1998) Toxin and subunit specificity of blocking affinity of three peptide toxins for heteromultimeric, voltage-gated potassium channels expressed in Xenopus oocytes - PubMed. J Pharmacol Exp Ther 285:1051–1060 Available at: https://pubmed.ncbi.nlm.nih.gov/9618407/ [Accessed May 31, 2024].

Keifman E, Ruiz-DeDiego I, Pafundo DE, Paz RM, Solís O, Murer MG, Moratalla R (2019) Optostimulation of striatonigral terminals in substantia nigra induces dyskinesia that increases after L-DOPA in a mouse model of Parkinson's disease. Br J Pharmacol 176:2146–2161 Available at: https://onlinelibrary.wiley.com/doi/abs/10.1111/bph.14663 [Accessed July 9, 2019].

Kharkwal G, Brami-Cherrier K, Lizardi-Ortiz JE, Nelson AB, Ramos M, Del Barrio D, Sulzer D, Kreitzer AC, Borrelli E (2016) Parkinsonism Driven by Antipsychotics Originates from Dopaminergic Control of Striatal Cholinergic Interneurons. Neuron 91:67–78 Available at: http://linkinghub.elsevier.com/retrieve/pii/S0896627316302677 [Accessed January 2, 2018].

Kimura M, Rajkowski J, Evarts E (1984) Tonically discharging putamen neurons exhibit set-dependent responses. Proc Natl Acad Sci U S A 81:4998–5001 Available at: http://www.ncbi.nlm.nih.gov/pubmed/6589643 [Accessed January 24, 2018].

Krok AC, Maltese M, Mistry P, Miao X, Li Y, Tritsch NX (2023) Intrinsic dopamine and acetylcholine dynamics in the striatum of mice. Nature 621:543–549 Available at: https://pubmed.ncbi.nlm.nih.gov/37558873/ [Accessed May 31, 2024].

Matsumoto N, Minamimoto T, Graybiel AM, Kimura M (2001) Neurons in the thalamic CM-Pf complex supply striatal neurons with information about behaviorally significant sensory events. J Neurophysiol 85:960–976 Available at: http://www.ncbi.nlm.nih.gov/pubmed/11160526 [Accessed November 12, 2014].

McGuirt A, Pigulevskiy I, Sulzer D (2022) Developmental regulation of thalamus-driven pauses in striatal cholinergic interneurons. iScience 25 Available at: https://pubmed.ncbi.nlm.nih.gov/36325074/ [Accessed May 31, 2024].

McKinley JW, Shi Z, Kawikova I, Hur M, Bamford IJ, Sudarsana Devi SP, Vahedipour A, Darvas M, Bamford NS (2019) Dopamine Deficiency Reduces Striatal Cholinergic Interneuron Function in Models of Parkinson's Disease. Neuron 103:1056-1072.e6 Available at: https://pubmed.ncbi.nlm.nih.gov/31324539/ [Accessed May 31, 2024].

Paxinos G, Franklin K (2001) The mouse brain in stereotaxic coordinates. San Diego: Academic Press.

Paz RM, Stahl AM, Rela L, Murer MG, Tubert C (2022) D1/D5 Inverse Agonists Restore Striatal Cholinergic Interneuron Physiology in Dyskinetic Mice. Mov Disord 37:1693–1706.

Paz RM, Tubert C, Stahl A, Díaz AL, Etchenique R, Murer MG, Rela L (2018) Inhibition of striatal cholinergic interneuron activity by the Kv7 opener retigabine and the nonsteroidal anti-inflammatory drug diclofenac. Neuropharmacology 137.

Paz RM, Tubert C, Stahl AM, Amarillo Y, Rela L, Murer MG (2021) Levodopa Causes Striatal Cholinergic Interneuron Burst-Pause Activity in Parkinsonian Mice. Mov Disord.

Reynolds JNJ, Avvisati R, Dodson PD, Fisher SD, Oswald MJ, Wickens JR, Zhang YF (2022) Coincidence of cholinergic pauses, dopaminergic activation and depolarisation of spiny projection neurons drives synaptic plasticity in the striatum. Nat Commun 13 Available at: https://pubmed.ncbi.nlm.nih.gov/35277506/ [Accessed May 31, 2024].

Reynolds JNJ, Hyland BI, Wickens JR (2004) Modulation of an Afterhyperpolarization by the Substantia Nigra Induces Pauses in the Tonic Firing of Striatal Cholinergic Interneurons. J Neurosci 24:9870–9877 Available at: http://www.ncbi.nlm.nih.gov/pubmed/15525771 [Accessed January 19, 2018].

Sanchez G, Rodriguez MJ, Pomata P, Rela L, Murer MG (2011) Reduction of an afterhyperpolarization current increases excitability in striatal cholinergic interneurons in rat parkinsonism. J Neurosci 31:6553–6564 Available at: http://www.ncbi.nlm.nih.gov/pubmed/21525296 [Accessed February 5, 2015].

Schulz JM, Reynolds JNJ (2013) Pause and rebound: sensory control of cholinergic signaling in the striatum. Trends Neurosci 36:41–50 Available at: https://pubmed.ncbi.nlm.nih.gov/23073210/ [Accessed May 31, 2024].

Threlfell S, Lalic T, Platt NJ, Jennings KA, Deisseroth K, Cragg SJ (2012) Striatal dopamine release is triggered by synchronized activity in cholinergic interneurons. Neuron 75:58–64 Available at: http://www.ncbi.nlm.nih.gov/pubmed/22794260 [Accessed November 12, 2014].

Tubert C, Taravini IRE, Flores-Barrera E, Sánchez GM, Prost MA, Avale ME, Tseng KY, Rela L, Murer MG (2016) Decrease of a Current Mediated by K<inf>v</inf>1.3 Channels Causes Striatal Cholinergic Interneuron Hyperexcitability in Experimental Parkinsonism. Cell Rep 16.

Watanabe K, Kimura M (1998) Dopamine Receptor–Mediated Mechanisms Involved in the Expression of Learned Activity of Primate Striatal Neurons. J Neurophysiol 79:2568–2580 Available at: http://www.ncbi.nlm.nih.gov/pubmed/9582229 [Accessed January 25, 2018].

Wilson CJ (2005) The mechanism of intrinsic amplification of hyperpolarizations and spontaneous bursting in striatal cholinergic interneurons. Neuron 45:575–585 Available at: http://www.ncbi.nlm.nih.gov/pubmed/15721243 [Accessed April 21, 2015].

Wilson CJ, Goldberg JA (2006) Origin of the slow afterhyperpolarization and slow rhythmic bursting in striatal cholinergic interneurons. J Neurophysiol 95:196–204 Available at: http://www.ncbi.nlm.nih.gov/pubmed/16162828 [Accessed July 7, 2015].

Zhang B, Albaker A, Plouffe B, Lefebvre C, Tiberi M (2014) Constitutive activities and inverse agonism in dopamine receptors. Adv Pharmacol 70:175–214 Available at: https://pubmed.ncbi.nlm.nih.gov/24931197/ [Accessed March 21, 2023].

Zhang YF, Reynolds JNJ, Cragg SJ (2018) Pauses in Cholinergic Interneuron Activity Are Driven by Excitatory Input and Delayed Rectification, with Dopamine Modulation. Neuron 98:918-925.e3 Available at: https://pubmed.ncbi.nlm.nih.gov/29754751/ [Accessed May 31, 2024].

Figure legends

Figure 1: SCIN burst-pause response to activation of thalamic terminals. A. Experimental design. **B.** Micrograph showing the thalamic region transfected with ChR2-YFP (left) and a striatal region (z-stack maximal projection) showing tdTomato-reported SCIN and thalamic terminals expressing ChR2-YFP (right). **C.** Schematic representation of optogenetic stimulation of thalamic inputs to a SCIN recorded in cell-attached configuration. Picrotoxin (PIC, 100 uM; GABA-A antagonist) was present in the bath in all experiments. **D.** Representative recording of a SCIN that responded to optogenetic activation of thalamic terminals with 1 spike. Inset: Detail of the measurements of x1 and x2 values. x1: time from the last spike before the optogenetic stimulation and the start of the stimulation; x2: time from the initiation of stimulation to the following spike. **E.** x2/Baseline ISI vs x1/Baseline ISI for single spike responses to optogenetic activation of thalamic terminals (Nonlinear fit, R^2=0.06237; Pearson correlation *p=0.0034). **F.** Representative recordings of the pause response of a SCIN to optogenetic stimulation of thalamic terminals in cell-attached configuration before and after bath application of CNQX (20 uM; AMPA receptor antagonist). **G.** Pause duration/Baseline ISI of SCIN that responded with 1, 2, 3 or 4 spikes to optogenetic activation of thalamic terminals (One-way RM ANOVA, treatment 2 vs 3 spikes: *p=0.0032; 2 vs 4 spikes: *p=0.0017). **H.** Baseline ISI of SCIN that responded with 1, 2, 3 or 4 spikes to optogenetic activation of thalamic terminals (One-way RM ANOVA, ns). **I.** Representative recordings of SCIN stimulated with one train of optogenetic activation of thalamic terminals (top) or with two trains (bottom). **J.** Pause duration/Baseline ISI of SCIN that responded with 1, 2, 3 or 4 spikes to optogenetic activation of thalamic terminals, with one or two trains of stimulation pulses. The second train occurs 350 ms after the first train. (Two-way RM ANOVA, interaction ns; treatment *p<0.0001; Elicited spikes *p<0.0001; 2 vs 4 spikes *p=0.0042). Mean +/- SEM; n=11-18 cells per group, from >5 mice.

Figure 2: Contribution of the Kv1 current to the pause response. A. Schematic representation of the tested hypotheses. DP: depolarization; HP: hyperpolarization; Glu: glutamate; DA: dopamine. **B.** Representative recordings of SCIN in response to optogenetic activation of thalamic terminals, with or without Margatoxin (MgTx; Kv1.3 channel blocker) or dendrotoxin (DTx; Kv1.1 and Kv1.6 channels blocker) in the bath. **C.** Pause duration/Baseline ISI of SCIN that responded with 1, 2, 3 or 4 spikes to optogenetic activation of thalamic terminals, with or without MgTx 3nM, 30 nM, or DTx 100 nM, in the bath (Two-way RM ANOVA interaction ns, treatment *p=0.0051; Control-MgTx 30nM: *p=0.0005; Control-MgTx 3nM: ns; Control-DTX: *p=0.0462; MgTx 30nM-MgTx 3nM: *p<0.0001; MgTx 30nM-DTX: ns; MgTx 3nM-DTX: *p=0.0027). **D.** Baseline ISI of SCIN recorded with or without MgTx 3nM, 30 nM, or DTx (One-way ANOVA, ns). **E.** Burst duration of SCIN that responded with 2, 3 or 4 spikes to optogenetic activation of thalamic terminals, with or without MgTx 3nM, 30 nM or DTx 100 nM, in the bath (Two-way RM ANOVA, ns). **F.** Representative recordings of SCIN in response to optogenetic activation of thalamic terminals, with or without Ba^{2+} (10 uM; Kir2.2 channel blocker at this concentration) or XE 991 (10 uM; Kv7 channel blocker) in the bath. **G.** Pause duration/Baseline ISI of SCIN that responded with 1, 2, 3 or 4 spikes to optogenetic activation of thalamic terminals, with or without 10 uM XE 991 or 10 uM Ba^{2+} (Two-way RM ANOVA, ns). **H.** Baseline ISI of SCIN recorded with or without Ba^{2+} or XE 991 (One-way ANOVA, ns). **I.** Burst duration of SCIN

that responded with 2, 3 or 4 spikes to optogenetic activation of thalamic terminals, for the above conditions (Two-way RM ANOVA, ns). Mean +/- SEM; n=7-16 cells per group, from >5 mice.

Figure 3: Modulation of the pause response by dopamine receptors. A. Schematic representation of the tested hypotheses. DP: depolarization. **B.** Representative responses of SCIN to optogenetic activation of thalamic terminals, with SKF81297 (2 uM; D1/D5 selective agonist), SCH23390 (10 uM; D1/D5 selective antagonist) or SKF81297 + SCH23390 in the bath. **C.** Pause duration/Baseline ISI of SCIN that responded with 1, 2, 3 or 4 spikes to optogenetic activation of thalamic terminals, under the above conditions (Two-way RM ANOVA, interaction p=0.0381, Dunnett's multiple comparisons test: Control vs SKF81297: 3 spikes *p=0.0001; 4 spikes *p=0.0010.). **D.** Baseline ISI of SCIN that responded with 1, 2, 3 or 4 spikes to optogenetic activation of thalamic terminals, under the above conditions (One-way ANOVA, ns). **E.** Burst duration of SCIN that responded with 2, 3 or 4 spikes to optogenetic activation of thalamic terminals, under the above conditions (Two-way RM ANOVA, ns). **F.** Representative responses of SCIN to optogenetic activation of thalamic terminals, with Sulpiride (10 uM; D2-type receptor selective antagonist) or Mecamylamine (10 uM; nicotinic receptors antagonist) in the bath. **G.** Pause duration/Baseline ISI of SCIN that responded with 1, 2, 3 or 4 spikes to optogenetic activation of thalamic terminals, under the above conditions (Two-way RM ANOVA, interaction p=0.0369, Dunnett's multiple comparisons test: Control vs Sulpiride: 4 spikes *p=0.0056; Control vs Mecamylamine: 4 spikes *p=0.0167.). **H.** Baseline ISI of SCIN that responded with 1, 2, 3 or 4 spikes to optogenetic activation of thalamic terminals, under the above conditions (One-way ANOVA, ns). **I.** Burst duration of SCIN that responded with 2, 3 or 4 spikes to optogenetic activation of thalamic terminals, under the above conditions (Two-way RM ANOVA, ns). Mean +/- SEM; n=7-15 cells per group, from >5 mice.

Figure 4: D5R modulation independent of Ih current. A. Schematic representation of the tested hypotheses. **B.** Time matched representative responses of SCIN to hyperpolarizing current steps with or without ZD7288 (30 uM; HCN channel blocker) in the recording pipette, and with or without SKF81297 (2 uM; D1/D5 selective agonist) in the bath. **C.** Sag evaluated in the hyperpolarizing step, under the above conditions (One-way ANOVA), p<0.0001; Tukey's multiple comparisons test: Control vs ZD7288 *p<0.0001; Control vs ZD7288+SKF81297 *p<0.0001). **D.** Representative responses in whole cell configuration to optogenetic activation of thalamic terminals, under the above conditions. **E.** Pause duration/Baseline ISI of SCIN that responded with 1, 2, 3 or 4 spikes to optogenetic activation of thalamic terminals, under the above conditions (Two-way RM ANOVA, interaction ns, treatment p=0.0373; Control vs ZD7288+SKF81297: *p=0.0005; ZD7288 vs ZD7288+SKF81297: *p=0.0067). **F.** Baseline ISI of SCIN that responded with 1, 2, 3 or 4 spikes to optogenetic activation of thalamic terminals, under the above conditions (One-way ANOVA, ns). **G.** Burst duration of SCIN that responded with 2, 3 or 4 spikes to optogenetic activation of thalamic terminals, under the above conditions (Two-way RM ANOVA, ns). Mean +/- SEM; n=13/14 cells per group, from >5 mice.

Figure 5: SCIN from L-DOPA-treated parkinsonian mice show a reduced pause response. A. Experimental design. **B.** Micrographs showing TH immunostaining at the level of the substantia nigra. **C-E.** Rotation index (C), forelimb asymmetry (D) and latency to fall from the rotarod (E) for sham and 6-OHDA mice (C-D: unpaired t test, **p<0.0001; E: Two-way RM ANOVA, interaction: *p=0.0284, n=5 sham and 22 6-OHDA mice). **F.** Abnormal involuntary movement (AIM) score of chronically L-DOPA-treated 6-OHDA mice. (Two-way RM ANOVA, interaction: p=0.0081; post-hoc: Day 1 vs Day 4 *p<0.03). **G.** Representative cell-attached recordings of the pause response of SCIN to optogenetic stimulation of thalamic terminals, in a sham and a dyskinetic mouse in the OFF L-DOPA condition, with or without MgTx 30 nM in the bath. **H.** Pause duration/Baseline ISI of SCIN that responded with 1, 2, 3 or 4 spikes to optogenetic activation of thalamic terminals (Two-way RM ANOVA, interaction ns, treatment *p=0.0227; Sham vs OFF L-DOPA: *p=0.0301; OFF L-DOPA vs OFF L-DOPA+MgTx: ns; Sham vs OFF L-DOPA+MgTx: *p=0.0032). **I.** Baseline ISI of SCIN that responded with 1, 2, 3 or 4 spikes to optogenetic activation of thalamic terminals under the above conditions (One-way ANOVA, *p=0.0254; Sham vs OFF L-DOPA: *p=0.0201; OFF L-DOPA vs OFF L-DOPA+MgTx: ns; Sham vs OFF L-DOPA+MgTx: ns). **J.** Burst duration of SCIN that responded with 2, 3 or 4 spikes to optogenetic activation of thalamic terminals under the above conditions (Two-way RM ANOVA, ns). Mean +/- SEM; n=14-27 cells per group, from >5 mice.

Figure 6: D1-like receptors inverse agonist restores the pause response in SCIN from OFF L-DOPA parkinsonian mice. A. Schematic representation of the tested hypothesis. **B.** Representative responses of SCIN from OFF L-DOPA dyskinetic mice to optogenetic activation of thalamic terminals, with or without SKF81297, Clozapine (10 uM; D1/D5 receptor inverse agonist), SCH23390 (10 uM; D1/D5 selective antagonist), Clozapine + SCH23390 or Clozapine + MgTx, in the bath. **C.** Pause duration/Baseline ISI of SCIN from OFF L-DOPA dyskinetic mice that responded with 1, 2, 3 or 4 spikes to optogenetic activation of thalamic terminals (Two-way RM ANOVA, interaction *p=0.0489, Dunnett's multiple comparisons test: 4 elicited spikes: OFF L-DOPA vs Clozapine: *p=0.0181). **D.** Baseline ISI of SCIN that responded with 1, 2, 3 or 4 spikes to optogenetic activation of thalamic terminals, under the above conditions (One-way ANOVA, ns). **E.** Burst duration of SCIN from dyskinetic mice OFF L-DOPA that responded with 2, 3 or 4 spikes to optogenetic activation of thalamic terminals, under the above conditions (Two-way RM ANOVA, interaction ns, treatment ns). Mean +/- SEM; n=6-17 cells per group, from >5 mice. **F.** Schematic representation of conclusion. Left, in physiologic conditions the balance of D2 versus D5 activation emerges as a determinant of the Kv1-dependent pause expression; right, in parkinsonian mice an imbalance towards D5 signaling abolishes the pause (top), which can be reset with D5 inverse agonism (bottom).

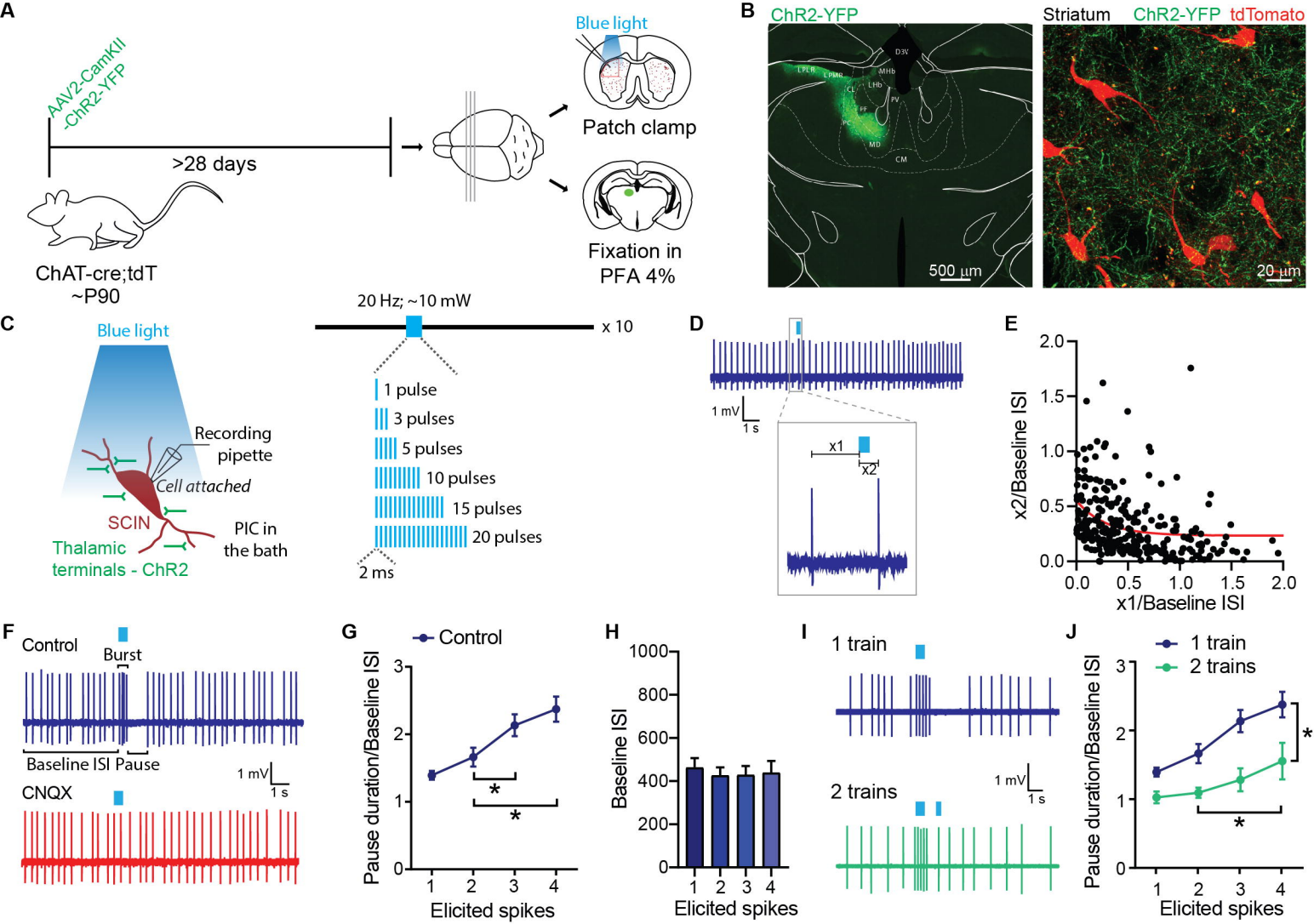
A
AAV2-CamKII -ChR2-YFP
>28 days
ChAT-cre;tdT ~P90
Blue light
Patch clamp
Fixation in PFA 4%
B
ChR2-YFP
Striatum
ChR2-YFP tdTomato
500 µm
20 µm
C
Blue light
Recording pipette
Cell attached
SCIN
PIC in the bath
Thalamic terminals - ChR2
20 Hz; ~10 mW
x 10
1 pulse
3 pulses
5 pulses
10 pulses
15 pulses
20 pulses
2 ms
D
1 mV
1 s
x1
x2
E
x2/Baseline ISI
x1/Baseline ISI
F
Control
Burst
Baseline ISI
Pause
1 mV
1 s
CNQX
G
Control
Pause duration/Baseline ISI
Elicited spikes
H
Baseline ISI
Elicited spikes
I
1 train
2 trains
1 mV
1 s
J
1 train
2 trains
Pause duration/Baseline ISI
Elicited spikes

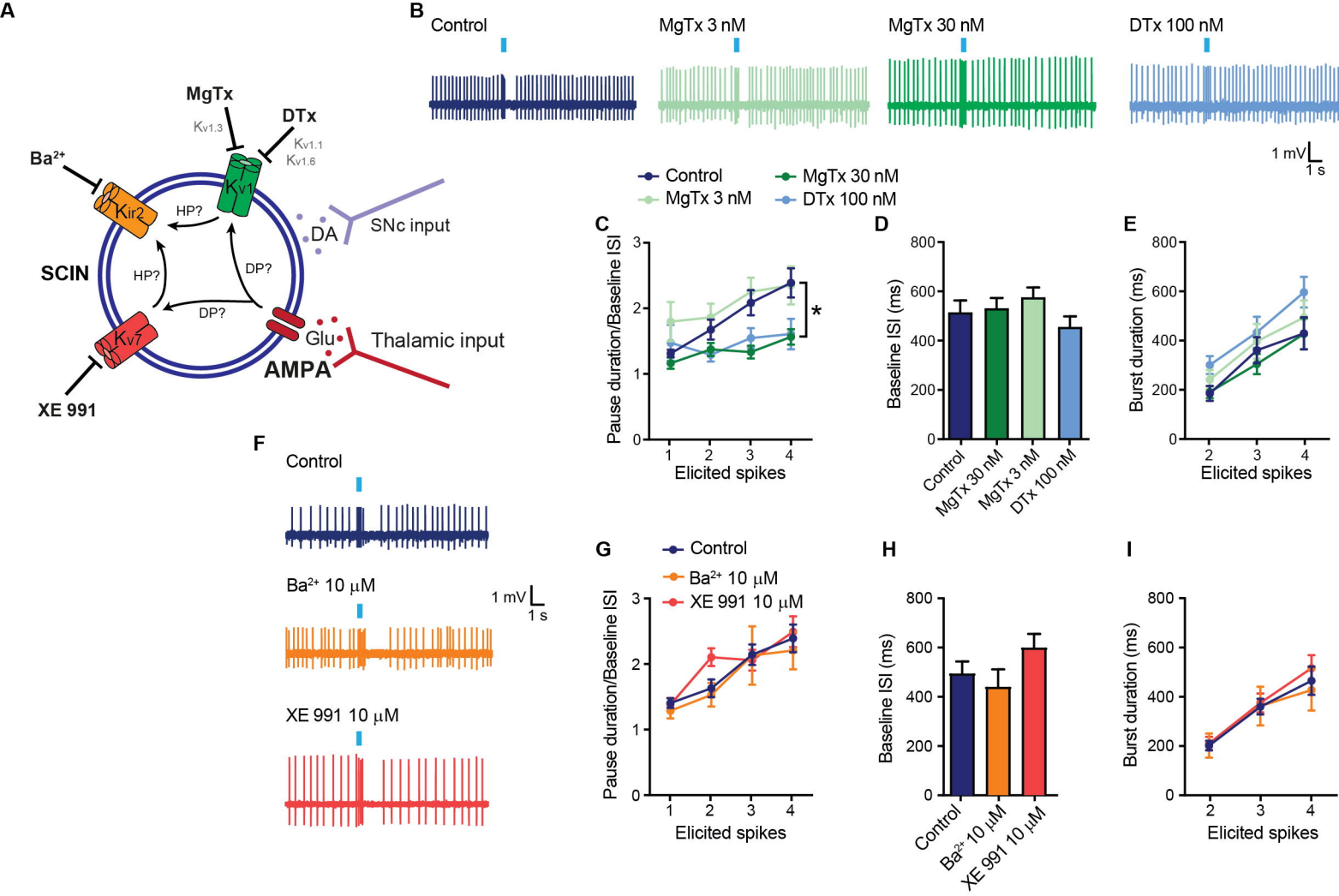
A
MgTx
Kv1.3
DTx
Kv1.1
Kv1.6
Ba2+
Kir2
Kv1
HP?
DA
SNc input
SCIN
HP?
DP?
DP?
Kv7
Glu
Thalamic input
AMPA
XE 991
B
Control
MgTx 3 nM
MgTx 30 nM
DTx 100 nM
1 mV
1 s
Control
MgTx 3 nM
MgTx 30 nM
DTx 100 nM
C
Pause duration/Baseline ISI
Elicited spikes
*
D
Baseline ISI (ms)
Control
MgTx 30 nM
MgTx 3 nM
DTx 100 nM
E
Burst duration (ms)
Elicited spikes
F
Control
Ba2+ 10 μM
1 mV
1 s
XE 991 10 μM
G
Control
Ba2+ 10 μM
XE 991 10 μM
Pause duration/Baseline ISI
Elicited spikes
H
Baseline ISI (ms)
Control
Ba2+ 10 μM
XE 991 10 μM
I
Burst duration (ms)
Elicited spikes

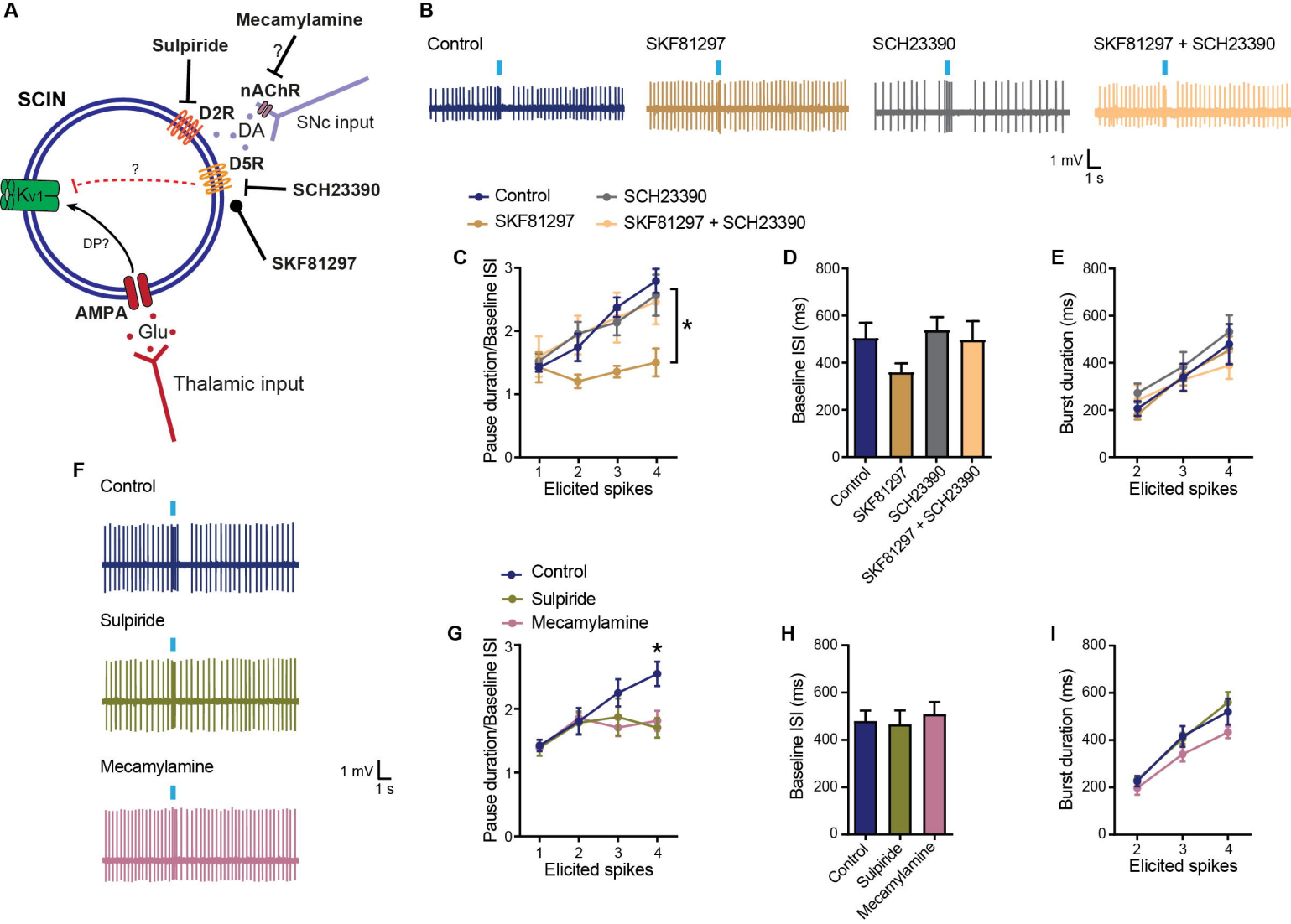
A
Mecamylamine
Sulpiride
?
nAChR
SCIN
D2R
DA
SNc input
D5R
?
Kv1
SCH23390
DP?
SKF81297
AMPA
Glu
Thalamic input
B
Control
SKF81297
SCH23390
SKF81297 + SCH23390
1 mV
1 s
Control
SCH23390
SKF81297
SKF81297 + SCH23390
C
Pause duration/Baseline ISI
Elicited spikes
*
D
Baseline ISI (ms)
Control
SKF81297
SCH23390
SKF81297 + SCH23390
E
Burst duration (ms)
Elicited spikes
F
Control
Sulpiride
Mecamylamine
1 mV
1 s
Control
Sulpiride
Mecamylamine
G
Pause duration/Baseline ISI
Elicited spikes
*
H
Baseline ISI (ms)
Control
Sulpiride
Mecamylamine
I
Burst duration (ms)
Elicited spikes

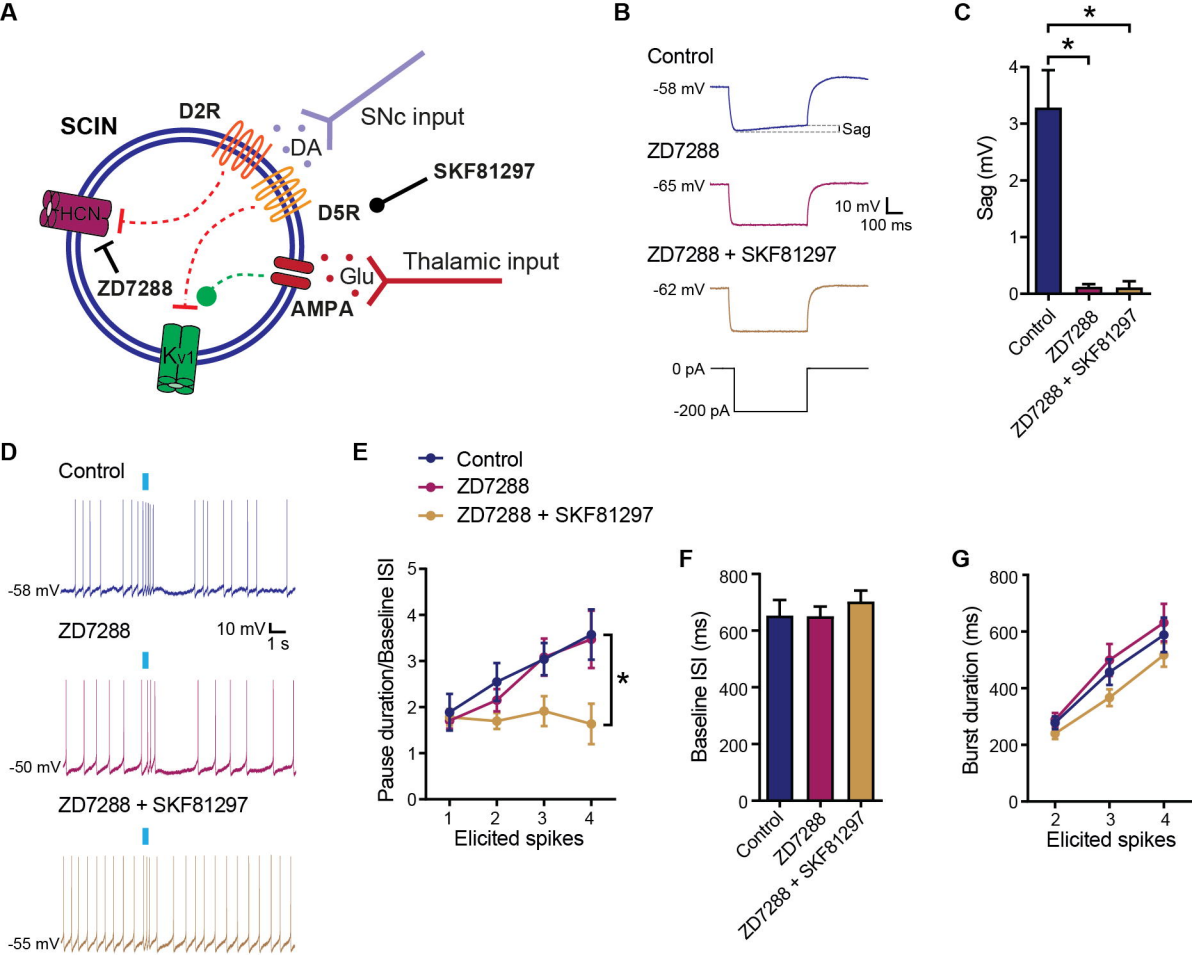
A
SCIN
D2R
DA
SNc input
SKF81297
D5R
HCN
ZD7288
Glu
Thalamic input
AMPA
Kv1
B
Control
-58 mV
Sag
ZD7288
-65 mV
10 mV
100 ms
ZD7288 + SKF81297
-62 mV
0 pA
-200 pA
C
Sag (mV)
Control
ZD7288
ZD7288 + SKF81297
D
Control
-58 mV
ZD7288
10 mV
1 s
-50 mV
ZD7288 + SKF81297
-55 mV
E
Control
ZD7288
ZD7288 + SKF81297
Pause duration/Baseline ISI
Elicited spikes
F
Baseline ISI (ms)
Control
ZD7288
ZD7288 + SKF81297
G
Burst duration (ms)
Elicited spikes

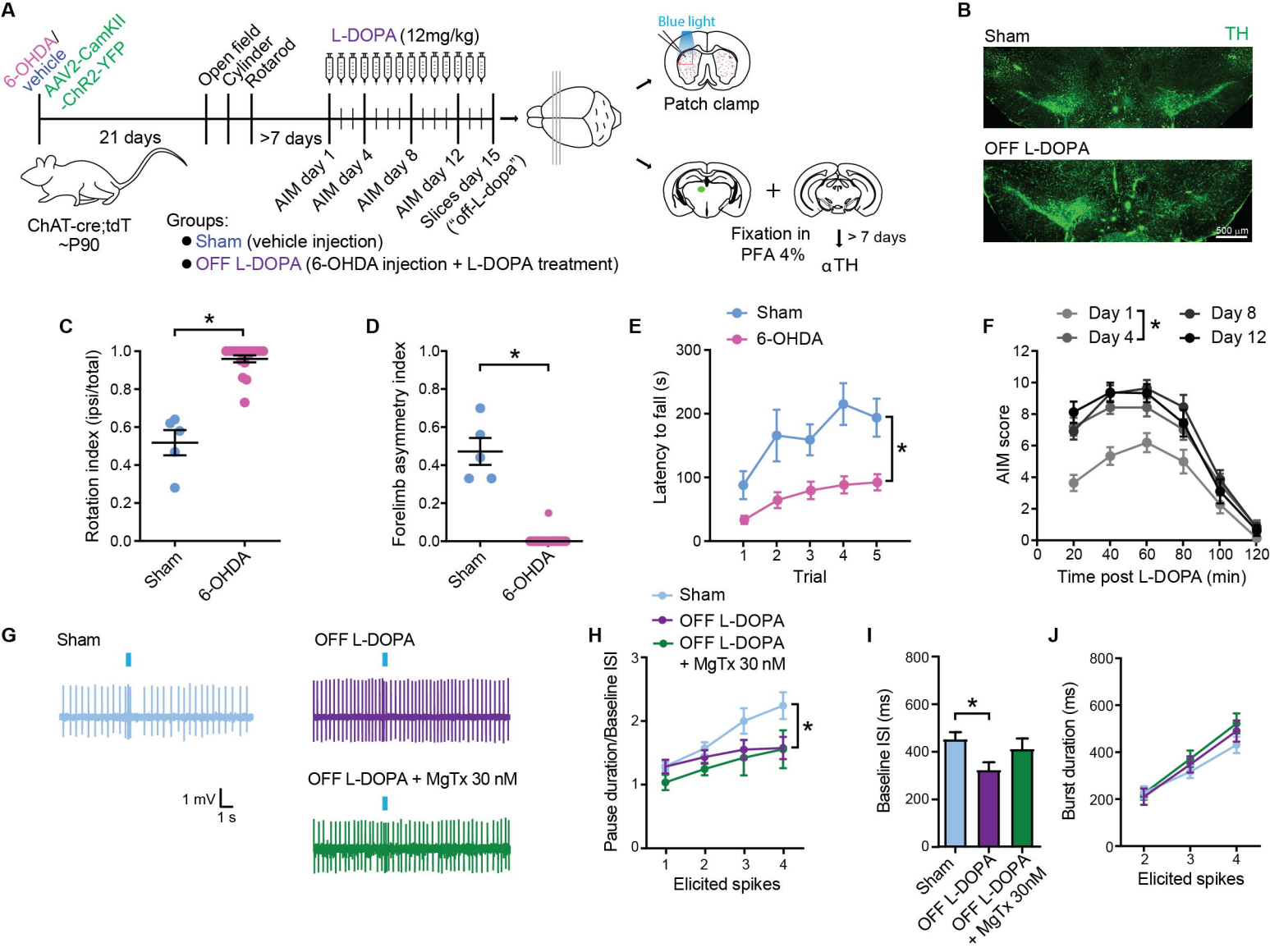
A
6-OHDA/ vehicle
AAV2-CamKII -ChR2-YFP
21 days
Open field
Cylinder
Rotarod
>7 days
L-DOPA (12mg/kg)
AIM day 1
AIM day 4
AIM day 8
AIM day 12
Slices day 15 ("off-L-dopa")
ChAT-cre;tdT ~P90
Groups:
Sham (vehicle injection)
OFF L-DOPA (6-OHDA injection + L-DOPA treatment)
Blue light
Patch clamp
Fixation in PFA 4%
> 7 days
αTH
B
Sham
TH
OFF L-DOPA
500 µm
C
Rotation index (ipsi/total)
Sham
6-OHDA
D
Forelimb asymmetry index
Sham
6-OHDA
E
Sham
6-OHDA
Latency to fall (s)
Trial
F
Day 1
Day 4
Day 8
Day 12
AIM score
Time post L-DOPA (min)
G
Sham
OFF L-DOPA
OFF L-DOPA + MgTx 30 nM
1 mV
1 s
H
Sham
OFF L-DOPA
OFF L-DOPA + MgTx 30 nM
Pause duration/Baseline ISI
Elicited spikes
I
Baseline ISI (ms)
Sham
OFF L-DOPA
OFF L-DOPA + MgTx 30nM
J
Burst duration (ms)
Elicited spikes

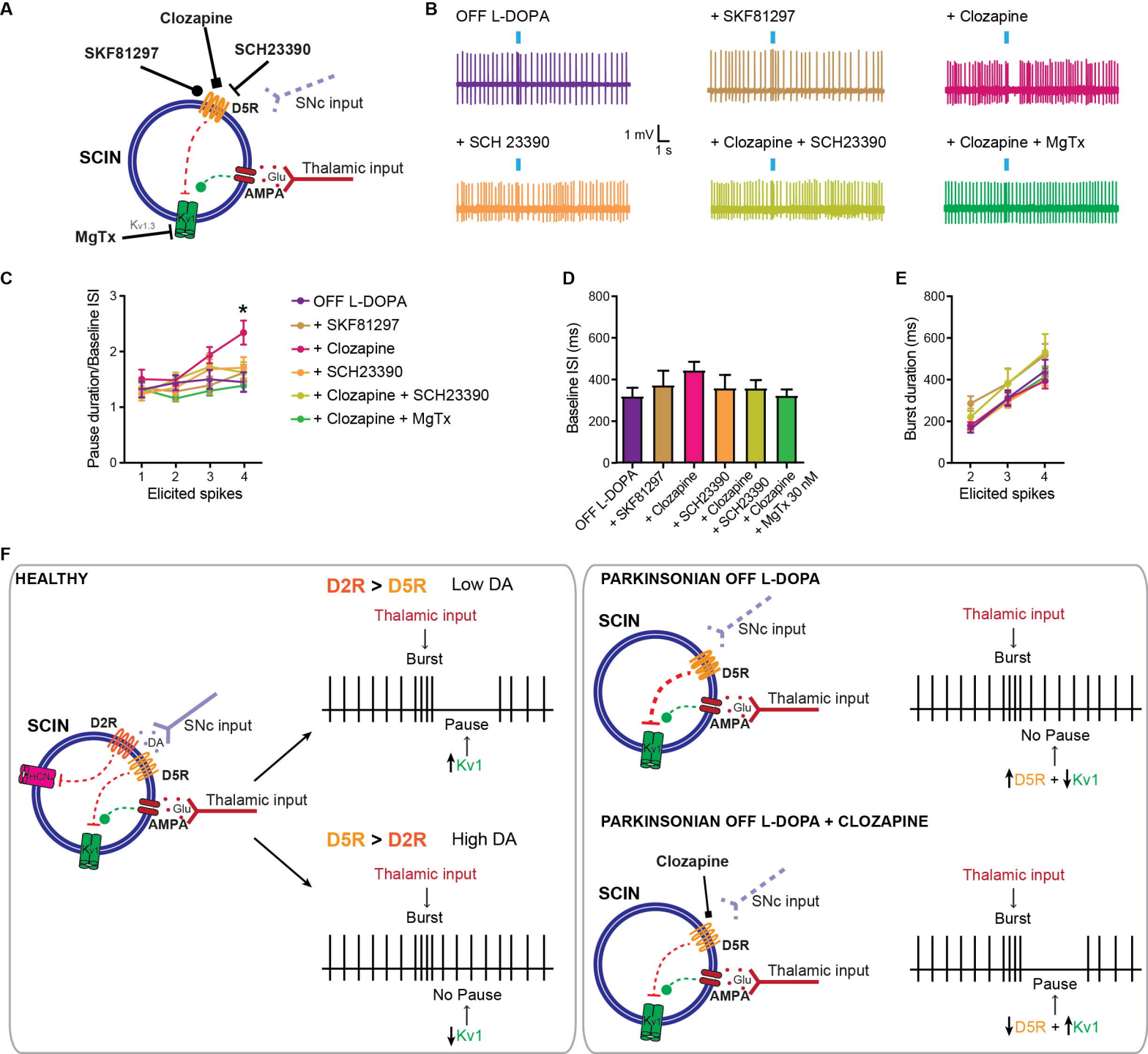
A
Clozapine
SKF81297
SCH23390
D5R
SNc input
SCIN
Thalamic input
Glu
AMPA
MgTx
Kv1.3
Kv1
B
OFF L-DOPA
+ SKF81297
+ Clozapine
+ SCH 23390
1 mV
1 s
+ Clozapine + SCH23390
+ Clozapine + MgTx
C
Pause duration/Baseline ISI
Elicited spikes
*
OFF L-DOPA
+ SKF81297
+ Clozapine
+ SCH23390
+ Clozapine + SCH23390
+ Clozapine + MgTx
D
Baseline ISI (ms)
OFF L-DOPA
+ SKF81297
+ Clozapine
+ SCH23390
+ Clozapine + SCH23390
+ Clozapine + MgTx 30 nM
E
Burst duration (ms)
Elicited spikes
F
HEALTHY
D2R > D5R
Low DA
Thalamic input
Burst
Pause
Kv1
SCIN
D2R
SNc input
DA
D5R
HCN
Glu
AMPA
Thalamic input
D5R > D2R
High DA
Thalamic input
Burst
No Pause
Kv1
PARKINSONIAN OFF L-DOPA
SCIN
SNc input
D5R
Glu
AMPA
Thalamic input
Thalamic input
Burst
No Pause
D5R + Kv1
PARKINSONIAN OFF L-DOPA + CLOZAPINE
Clozapine
SCIN
SNc input
D5R
Glu
AMPA
Thalamic input
Thalamic input
Burst
Pause
D5R + Kv1